

Conservative upper limits on WIMP annihilation cross section from Fermi-LAT γ -rays

Francesca Calore*

*II. Institute for Theoretical Physics, University of Hamburg,
Luruper Chaussee 149, 22761 Hamburg, Germany*

Valentina De Romeri†

*Astroparticle and High Energy Physics Group, IFIC (CSIC - Universidad de Valencia) - Edificio Institutos de Investigacion,
C/ Catedrático Jose Beltrán 2, E-46980 Paterna (Valencia), Spain*

Fiorenza Donato‡

Dipartimento di Fisica Teorica, Università di Torino and INFN, Via P. Giuria 1, 10122 Torino, Italy

The spectrum of an isotropic extragalactic γ -ray background (EGB) has been measured by the Fermi-LAT telescope at high latitudes. Two new models for the EGB are derived from the subtraction of unresolved point sources and extragalactic diffuse processes, which could explain from 30% to 70% of the Fermi-LAT EGB. Within the hypothesis that the two residual EGBs are entirely due to the annihilation of dark matter (DM) particles in the Galactic halo, we obtain stringent upper limits on their annihilation cross section. Severe bounds on a possible Sommerfeld enhancement of the annihilation cross section are set as well. Finally, we consider models for DM annihilation depending on the inverse of the velocity and associate the EGBs to photons arising from the annihilation of DM in primordial halos. Given our choices for the EGB and the minimal DM modelling, the derived upper bounds are claimed to be *conservative*.

PACS numbers: 95.30.Cq, 95.35.+d, 95.85.Pw, 96.50.sb

I. INTRODUCTION

The indirect search for dark matter (DM) through its annihilation products in rare charged cosmic rays (CRs) and in multi-wavelength channels requires very accurate measurements and an unambiguous estimation of all the possible backgrounds to the DM signal. In the last years, dedicated experiments have provided unprecedented results by extending the energy ranges of the measured cosmic species as well as the precision of the data [1–7]. Further data are expected by the Fermi-LAT and Pamela on-going missions, and by the AMS-02 experiment on board the International Space Station. From the theoretical side, many efforts have been addressed to a better and increasingly detailed modelization of the astrophysical processes which shape, at different levels, the observed fluxes. Data from cosmic antiprotons [5, 6] have been shown to be compatible with the standard production from CRs impinging on the interstellar gas [8]. The anomalous increasing positron fraction measured by Pamela [1, 2] and confirmed by Fermi-LAT [9] may be explained by emission from near pulsars over-imposed to a standard CR population [10, 11]. Alternatively, a DM component with very high cross section or sources concentration has been invoked [12–15]. Unprecedented γ -ray measurements by Fermi-LAT have boosted interpretation of diffused and point sources emission in terms

of exotic components from DM annihilation in the halo of the Milky Way, in extragalactic near objects or in cosmological structures [7, 16–18]. The very signature would be the monochromatic line, which nevertheless provides tiny signal on a remarkable background [19].

The high latitude γ -ray emission measured by Fermi-LAT [7], given its reduced contamination by galactic sources, can be a powerful tool to set limits on the contribution of DM to the measured flux. The data are indeed the result of a non trivial subtraction procedure and show a high isotropic feature.

The aim of the present research is to set *conservative* upper limits on the galactic weakly interacting massive particle (WIMP) DM annihilation cross section into γ -rays. We will confront the γ -rays coming both from the DM halo and high-redshift protohalos with the background observed by Fermi-LAT at high latitudes. The conservative approach is achieved - in addition to prudent assumptions on the particle physics model and DM distribution in the Galaxy - through the comparison of the putative DM signal with a high latitude diffuse emission spectrum (i.e. EGB) obtained with minimal subtractions of known unresolved sources.

Our paper proceeds as follows. In Sect. 2 we discuss the possible contributions to the high latitude γ -ray emission from unresolved point sources and truly diffuse processes. We subtract the non-negligible fluxes to the Fermi-LAT data and draw two possible scenarios for the high latitude emission. In Sect. 3 we derive conservative upper limits to the DM annihilation cross section by identifying the residual γ -ray flux with γ -rays from DM annihilation in the galactic halo and in primordial DM small halos at high redshift. In the latter case, we study models in

*Electronic address: francesca.calore@desy.de

†Electronic address: deromeri@ific.uv.es

‡Electronic address: donato@to.infn.it

which the DM annihilation cross section has an explicit dependence on the inverse of the velocity. We discuss also a possible Sommerfeld enhancement of the annihilation cross section and derive limits on its amplitude. In Sect. 4 we draw our conclusions.

II. THE EXTRAGALACTIC γ -RAY BACKGROUND

A diffuse γ -ray emission has been measured by the Fermi-LAT detector at high latitudes ($|b| > 10^\circ$) [7]. The spectrum has been obtained after the subtraction from the data of the sources resolved by the telescope, the (indeed model dependent) diffuse galactic emission, the CR background in the detector and the solar γ -ray emission. The resulting flux decreases with a power law of the photon energy with spectral index 2.41 ± 0.05 . It shows a highly isotropic sky distribution and is generically classified as an extragalactic γ -ray background (EGB).

The 1451 sources listed in this First Fermi-LAT catalog (1FGL) [20] represent the best-resolved survey of the sky in the 100 MeV to 100 GeV energy range. Out of the 1FGL 1451 sources, 821 (56%) have been associated with at least one non- γ -ray counterpart. The largest population is constituted by Active Galactic Nuclei (AGNs), mainly blazar candidates, with 685 associations. For each low-flux source there may be a large number of *unresolved* point sources which have not been detected because of selection effects (e.g. the local background was too large or the photon index was too soft, or a combination of both), or too low emission. Ref. [21] presents a study of the high latitude sources which have not been detected by Fermi-LAT because of these selection effects, but have a flux which is formally larger than the faintest detected source. The maximum contribution (arising from the integration of the logN-logS distribution down to zero flux) of unresolved sources to the diffuse background is estimated to be $2.39(\pm 0.48) \cdot 10^{-6}$ ph cm $^{-2}$ s $^{-1}$ sr $^{-1}$, which represents 23(± 5)% of the Fermi-LAT high latitude isotropic diffuse background [7].

Several possible sources to the residual EGB have been explored in the literature. From the analysis in Ref. [21], it is likely that most of unassociated high latitude sources are blazars and their pile to the EGB with the largest flux. Galactic resolved pulsars and Milli-Second Pulsars (MSPs) represent the second largest population in the Fermi-LAT catalog [20, 22] and they are expected to contribute significantly to the putative EGB. A non-negligible γ -ray flux seems to be guaranteed by unresolved normal star-forming galaxies [23]. Ultra-high energy CRs (UHECRs) may induce secondary electromagnetic cascades, originating neutrinos and γ -rays at Fermi-LAT energies [24]. All of these possible bricks to the residual EGB will be discussed in some detail in the following of this Section. Only contributions from unresolved blazars and MSPs are believed to contribute at least few percent to the Fermi-LAT EGB, while predic-

tions for star-forming galaxies and UHECRs are highly model dependent.

Several high latitude γ -ray sources have been explored and shown to contribute to less than about 1% of the Fermi-LAT EGB and/or to be too highly model dependent to firmly establish and subtract their contribution to the Fermi-LAT EGB. We list the main ones:

i) Radio-quiet AGN: γ -ray emission is supposedly produced by non-thermal electrons present in the corona above the accretion disk, but their contribution is still strongly uncertain because of the lack of observational evidences [25, 26].

ii) BL Lacs and FSRQs whose jets are not aligned along the line of sight (l.o.s.) constitute the Fanaroff and Riley radio galaxies of type I (FRI) and II (FRII), respectively. The kpc-scale jets in these misaligned radio galaxies can be a source of inverse Compton (IC) γ -ray emission. Fermi-LAT has detected 7 FRI and 4 FRII radio galaxies [27]. The FRI contribution to the EGB has been estimated to be about 1% of the EGRET observed EGB [28]. Recently, Ref. [29] estimates the possible γ -ray flux from 10 of the misaligned AGNs detected by Fermi-LAT, extrapolating the γ -ray luminosity from the radio-luminosity. Given the high uncertainty in the model, and noticed that all LAT detected sources were subtracted from the EGB measurement [7], the unresolved FRI and FRII radio galaxies contribution to the EGB is likely bound to few percent.

iii) The contribution of γ -ray bursts (GRBs) to the GeV extragalactic diffuse γ -ray flux (EGRET data), possibly due to a low energy synchrotron spectrum and a higher energy IC spectrum, has been shown to be tiny. In Ref. [30], it is estimated that less than 1% of the diffuse extragalactic γ -ray background could come from GRBs.

iv) The star-burst and luminous infrared galaxies, having gas densities and star formation rates higher than a factor of ten with respect to the Milky Way, may produce γ -ray photons in hadronic reactions. Fermi-LAT has detected the first high-energy γ -ray emission from two star-burst galaxies (M82 and NGC253) [31]. The relevant flux may cover a significant fraction of the EGB ($\leq 20\%$) [32], but the model dependence is such to prevent firm statements on the relevance of this extragalactic source.

v) γ -ray emission is also expected from nearby clusters of galaxies, even if in the first 18 months, Fermi-LAT has detected no γ -ray emission from such sources. The contribution from π^0 decays, IC scattering and ultra high energy (UHE) protons in the intra-cluster medium could yield about 1% – 10% of the EGRET EGB [33–35].

vi) Gravitational induced shock waves, produced during cluster mergers and large-scale structure formation, may give rise to highly relativistic electrons that are responsible for IC scattering of the cosmic microwave background (CMB) photons to GeV energies. A contribution to the γ -ray background is produced in filaments, sheets, and extended γ -ray halos associated with massive clusters. The estimation of the fluxes is quite model dependent and may reach few percent [36, 37].

All the γ -ray sources listed above for the sake of completeness will be neglected in rest of our paper because effectively negligible or too highly model dependent. In the following, we describe few classes of γ -ray emitters whose unresolved flux is firmly estimated in a non-negligible Fermi-LAT EGB percentage. In a conservative scenario (Model I), we will subtract AGN and MSPs to the Fermi-LAT EGB as derived in Ref. [7]. A more relaxed model (Model II) will be drawn by the further subtraction of a minimal flux from star-forming galaxies and CRs at the highest energies.

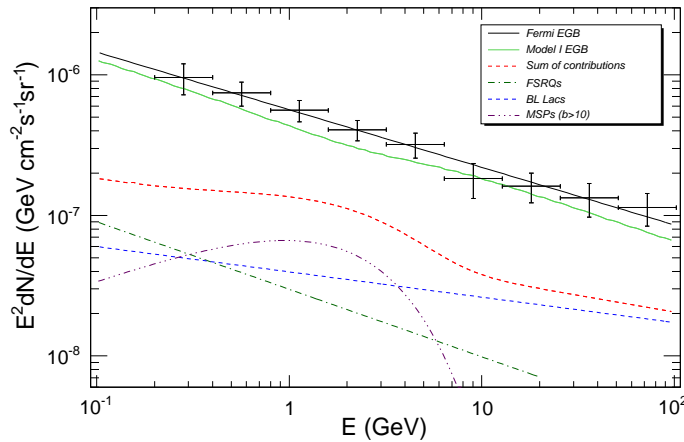


FIG. 1: γ -ray spectrum for $|b| > 10^\circ$ latitudes. Fermi-LAT data points are displayed along with their power-law fit (solid black curve) [7]. The dotted (blue), dot-dashed (green) and double dot-dashed (purple) curves correspond to BL Lacs, FSRQs and MSPs contribution, respectively. The dashed (red) curve is the sum of the previous three fluxes. The solid (lower, green) curve is derived by subtracting the three contributions to the Fermi-LAT result (Model I).

1. BL Lacs and FSRQs

An AGN is a compact region at the center of a galaxy, probably originated by galactic matter accretion onto a super-massive black hole. The released large amount of gravitational energy flows away through powerful jets of relativistic particles which in turn produce X and γ radiation. Blazars are those AGNs for which the jets are close to the l.o.s. The blazars classification includes BL Lacs, which present a complete or nearly complete lack of emission lines, and FSRQs. Blazars constitute the class of γ -ray emitters with the largest number of identified members. Therefore, unresolved blazars are expected to have a sizable contribution to the EGB, as already pointed out in Ref. [38]. The largest uncertainties in determining the blazars contribution are their unknown spectral energy distribution (SED) and luminosity function. Theoretical estimations of the γ -ray flux from unresolved FSRQs are

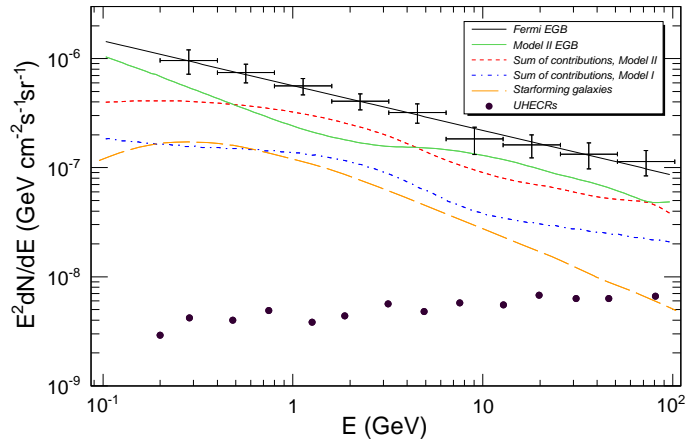


FIG. 2: γ -ray spectrum for $|b| > 10^\circ$ latitudes. Fermi-LAT data points are displayed along with their power-law fit (solid black curve) [7]. Dots and long dashed-curve (light blue) correspond to the UHECRs and star-forming galaxies γ -ray fluxes, respectively. The short-dashed (red) curve corresponds to the sum of BL Lacs, FSRQs and MSPs contribution (see Fig. 1), the short-dashed (blue) to the sum of the previous components with the star-forming galaxies and UHECRs ones. The solid (lower, green) curve is derived by subtracting all the contributions to the Fermi-LAT result (Model II).

derived in Ref. [39]. Adopting a power law γ -ray energy spectrum and assuming that the γ -ray luminosity of an FSRQ is, on average, proportional to its radio luminosity, the authors find that a scenario in which the EGB is dominated by emission from unresolved blazars is compatible with the Fermi source count data. In Ref. [26] it was shown that the EGB flux could be composed of blazars and non-blazar AGNs in the luminosity-dependent density evolution (LDDE) SED blazar model, consistently with the EGRET blazar data and the X-ray AGN surveys. Different models for the γ -ray luminosity function have been considered, as well different model parameters for the non-blazars γ -ray emission, leading to different theoretical predictions

In addition to phenomenological predictions largely affected by systematic and theoretical uncertainties, an analysis of the observed source count distribution through Monte Carlo simulations can determine the EGB contribution of an unresolved source class. In Ref. [21] the source count distribution of blazar objects in a simulated sample has been performed. The reliability of the Monte Carlo simulation and the detection algorithm relies onto a good agreement with the real data, from the comparison of reconstructed γ -ray fluxes and spectral properties of the sources. Notably, the number of identified simulated sources does not exceed the observed sample. The simulated contribution of unresolved FSRQs and BL Lacs to the EGB is reported in Fig. 20 of Ref. [21]. It is ob-

tained by integrating the simulated unresolved source count distribution from the flux of the faintest source in their sample ($S_{min}^{BL Lac} = 9.36 \cdot 10^{-10} \text{ ph cm}^{-2} \text{ s}^{-1}$ and $S_{min}^{FSRQ} = 1.11 \cdot 10^{-8} \text{ ph cm}^{-2} \text{ s}^{-1}$) to a maximal flux intensity $S_{max} = 10^{-3} \text{ ph cm}^{-2} \text{ s}^{-1}$. The energy spectrum is well described by a power-law for both the populations. FSRQs spectrum results softer than BL Lacs one, being the intersection between the two fluxes at about 400 MeV. Following our conservative approach - which is meant to consider the minimum unavoidable contribution to the EGB from unresolved astrophysical sources - we will adopt blazar contributions from the curves delimiting the lower uncertainty bands displayed in Fig. 20 of Ref. [21]. The ensuing flux is displayed in our Fig. 1 as dotted (dot-dashed) line for BL Lacs (FSRQs) contribution.

2. Pulsars and MSPs

As a result of their short periods, typical MSPs may be brighter in the γ -rays than ordinary pulsars [40]. MSPs have a characteristic age, extrapolated from their period and period-derivative, indicating that these objects are much older than ordinary pulsars. On the contrary young, energetic ordinary pulsars are more concentrated close to the Galactic plane, where they were born. The ages of MSPs generally exceed the oscillation time across the galactic disk by a large factor so that MSPs are expected to be more prevalent at high latitudes. In the first year of Fermi-LAT observations [20], 63 pulsars have been identified. Among them: (i) 16 pulsars at $|b| > 10^\circ$, of which 11 are MSPs; (ii) 5 MSPs at $|b| > 40^\circ$ and (iii) 1 MSP at $|b| > 60^\circ$. The empirical analysis conducted in Ref. [40] finds the γ -ray flux distribution of MSPs (i.e. the logN-logS distribution) to be close to Euclidean (i.e. homogeneous spatial distribution in a three-dimensional space) at the high end of the logN-logS flux distribution, in contrast to the ordinary γ -ray pulsars which are essentially found in the galactic disk.

We estimate a minimal but not negligible contribution of the unresolved MSPs population to the γ -ray flux at high latitudes. Concerning the emission energy spectrum, we adopt an empirical prescription outlined in Ref. [41], which is based on the spectra of the eight MSPs detected by Fermi in the first 9 months [42] of operation. The differential energy spectra of the Fermi-detected MSPs are well described by a truncated power law:

$$\frac{dN}{dE} = K E^{-\Gamma} e^{-E/E_{cut}}. \quad (1)$$

Γ and E_{cut} are assumed to be normally distributed in the MSP population with $\langle \Gamma \rangle = 1.5$ and $\langle E_{cut} \rangle = 1.9$ GeV. The normalization of the average intensity spectrum K has been obtained by averaging over 10 Monte Carlo realizations of galactic MSP population, generated by creating mock MSP catalogs and using a mask excluding $|b| \leq 40^\circ$.

In order to evaluate Eq. (1) for different observational regions - namely changing the normalization K - we follow the prescriptions given in Ref. [40]. Assuming a disk-like latitude profile, the ratio of the average intensities at different latitudes is given by:

$$\frac{I_{MSP}(|b| \geq b_1)}{I_{MSP}(|b| \geq b_2)} = \frac{\ln[(\sin|b_1|)^{-1}]}{\ln[(\sin|b_2|)^{-1}]}, \quad (2)$$

where $I_{MSP}(|b| \geq b_i)$, $i = 1, 2$, is the average MSP intensity over a solid angle $\Omega = 4\pi(1 - \sin|b_i|)$ defined by the integration from the minimal latitude b_i up to 90° , written as:

$$I_{MSP} \equiv \frac{S_{tot}}{\Omega} = \frac{S_{min}}{\Omega} \cdot \left(\frac{\delta - 1}{\delta - 2} \right) \cdot \left(\frac{S_{min}}{S_{th}} \right)^{1-\delta} \cdot N(S > S_{th}). \quad (3)$$

S_{min} refers to the assumed Euclidean logN-logS flux distribution of the galactic MSP population, which is parametrized by a power-law with spectral index $\delta = 2.5$ for $S \geq S_{min}$. According to [40], we set $S_{min} = 10^{-10} \text{ ph s}^{-1} \text{ cm}^{-2}$. $N(> S_{th})$ is the number of resolved sources above a given flux threshold S_{th} . We update the estimation for I_{MSP} in Ref. [40] with the more recent observations for $|b| \geq 10^\circ$ reported in Ref. [42], where 8 MSPs have been found above $S_{th} = 2 \cdot 10^{-8} \text{ ph s}^{-1} \text{ cm}^{-2}$ (lowest detected MSP flux). We find:

$$I_{MSP}(|b| \geq 10^\circ, E > 100 \text{ MeV}) = 6.54 \cdot 10^{-7} \text{ cm}^{-2} \text{ s}^{-1} \text{ sr}^{-1}. \quad (4)$$

K then is derived from:

$$I_{MSP} = \int_{E_{min}}^{E_{max}} \frac{dN}{dE} dE, \quad (5)$$

where $\frac{dN}{dE}$ refers to Eq. (1). Cross-checking the average MSP intensities obtained with the prescription outlined above, and the results in Ref. [41] for $|b| \geq 40^\circ$, we find a relative difference of about 30%, due to the theoretical uncertainties on the assumed logN-logS and the latitude profile. We consider such a discrepancy as an empirical theoretical uncertainty on the determination of K , and fix the unresolved MSPs contribution subtracting a 30% uncertainty from the estimated average intensity. The so derived contribution is shown in Fig. 1 as a double dot-dashed line.

3. Star-forming Galaxies

Unresolved normal star-forming galaxies are expected to give a guaranteed contribution to the high latitude isotropic diffuse γ -ray background. Fermi-LAT has identified the source of the diffuse emission from our Galaxy due to the collisions of CRs with interstellar gas, leading to γ -rays from π^0 decay in flight. This observation provides a ground to estimate the γ -ray luminosity of star-forming galaxies, by scaling the CR flux with the massive star formation rate and fixing the amount of the gas in the external galaxy.

The lack of statistics does not allow a source count population study for this source class. Several models rely on the determination of the γ -ray luminosity function describing the evolution of space density and luminosity with the redshift [23, 39, 43]. Those predictions are greatly affected by observational and theoretical uncertainties in the determination of the star formation rate of the galaxies and their gas content. Given the uncertainty surrounding key elements of the determination of this contribution, in our strictly conservative approach we do not take into account this component. We extend our analysis adopting a more relaxed perspective where also star-forming galaxies contribute.

As explained in Ref. [23], the γ -ray intensity depends on the average γ -ray luminosity evaluated at redshift $z=0$ and evolved with redshift over the distribution of star-forming galaxies. As it is unclear whether and how each parameter of the star-forming model evolves with the redshift, two limiting cases bracket the possible behaviours of the star-forming luminosity as a function of different cosmic star formation rates: pure luminosity evolution - the comoving density of stars is fixed - or pure density evolution - predicts an increase in the number of star-forming galaxies with the redshift. We consider the lowest predicted contribution from star-forming galaxies, i.e. the pure density evolution model as outlined in Ref. [23]. The adopted emission corresponds to the long dashed curve in Fig. 2.

4. UHECRs

UHECRs accelerated in astrophysical objects produce secondary electromagnetic cascades during their propagation in the cosmic microwave and infrared backgrounds. Ref. [24] shows that if the primary CRs are dominated by protons, such cascades can contribute between 1% and 50% of the GeV-TeV diffuse photon flux measured by the EGRET experiment. In Ref. [44], the EGB spectrum from UHECRs has been obtained through a Monte Carlo simulation of the cascade development and compared with the measurement of the EGB by Fermi-LAT. Assuming an injection spectrum in the form $dN/dE \propto E^{-\alpha_g}$ and a homogeneous source distribution up to a maximal redshift, UHE accelerated protons are propagated through the extragalactic space until their energy is below the threshold for e^+e^- pair production, $E_{min} \simeq 10^{18}$ eV, or until they reach the Earth. The simulation is performed for two UHECR models, corresponding to a different exponent of the generation spectrum: i) $\alpha_g = 2.6$ gives the cascade flux for the non-evolutionary dip model with maximal energy of acceleration $E_{max} = 1 \cdot 10^{21}$ eV and maximal redshift $z_{max} = 2$, while ii) $\alpha_g = 2.0$ represents the ankle model with a transition from galactic to extragalactic CRs at $5 \cdot 10^{18}$ eV, for the same values of E_{max} and z_{max} . The UHE proton fluxes are normalized to the HiRes data. From [44], we quantified the contribution of the two simulations to the

Fermi-LAT EGB intensity integrated above 200 MeV: it sets to 1.4 % for the non-evolutionary dip model, and to a mere 0.5 % for the ankle model. In our more relaxed, whether conservative scenario, we will subtract the ankle model contribution to the Fermi-LAT EGB, which we shown in Fig. 2.

A. Models for the EGB

As a result of the previous analysis, we have subtracted additional contributions to the Fermi-LAT EGB [7] at latitudes $|b| > 10^\circ$. In what we label Model I, we subtract the unresolved contributions for both BL Lacs and FSRQs as outlined in Sect. II 1, and the unresolved MSPs flux obtained according to the prescription Sect. II 2. We believe that these contributions are physical and must be accounted for in the γ -ray EGB spectrum. They are therefore included but considering the lower prediction at their charge. The results are shown in Fig. 1, where the Fermi-LAT EGB data are shown along with the power-law fit as reported in Ref. [7]. The contributions from BL Lacs, FSRQs and MSPs are identified by dotted, dot-dashed and double dotted-dashed curves, respectively. The fluxes from the blazar populations follow power-laws, with softer (harder) spectrum for the FSRQs (BL Lacs). The crossing point for the two curves is around 300 MeV: above this energy BL Lacs flux dominates over the FSRQs one. The γ -rays from unresolved MSPs show a peculiar spectrum peaked at about 1 GeV and dominate over the blazar spectra from 300 MeV up to 3-4 GeV. The sum of the three contributions reflects the MSPs flux shape with a mild bump. At about 100 MeV the three sources explain 10% of the Fermi-LAT EGB and 30% above 1 GeV. The residual flux, obtained by subtracting the sum of the three contributions (dashed curve) to the Fermi-LAT flux is identified by the lower solid curve. It is not a net power law due to the dip in the GeV region introduced by the MSPs flux.

Fig. 2 refers to the scenario where the additional contributions from star-forming galaxies (long dashed line) and UHECRs (solid points) as outlined in Sect. II 3 and Sect. II 4 add to explaining the Fermi-LAT EGB. We display the sum of the contributions this scenario (dashed line): blazar and MSPs (Model I), plus star-forming galaxies and UHECRs. The solid (green) curve derives from the subtraction of all these contributions from the Fermi-LAT EGB (solid black line fitting the data points) and is labelled Model II hereafter. Notably, the contribution from star-forming galaxies turns out to be relevant for $E \leq 1$ GeV, whereas the γ -rays from UHECRs give non-negligible fluxes only at the high-end of the energy spectrum. We notice that at 100 MeV Model II explains about 70% of the Fermi-LAT EGB, while above 1-2 GeV they count about 50% of the total. To consider additional astrophysical components to the EGB further decreases the residual flux (lower solid line) with respect to the Fermi-LAT EGB (upper solid line) and shrinks the room

left to potential exotic sources, like DM annihilations.

III. UPPER BOUNDS ON DM ANNIHILATION CROSS SECTION

In this Section we derive conservative upper limits on the WIMP annihilation cross section. We make the hypothesis that the residual fluxes we have derived in Sect. II A are entirely provided by the γ -rays produced by thermalized WIMP DM in the halo of the Milky Way.

A. γ -rays from DM annihilation

The flux of γ -rays $\Phi_\gamma(E_\gamma, \psi)$ originated from WIMP pair annihilation in the galactic halo [45–47] and coming from the angular direction ψ is given by:

$$\Phi_\gamma(E_\gamma, \psi) = \frac{1}{4\pi} \frac{\langle\sigma v\rangle}{m_\chi^2} \frac{dN_\gamma}{dE_\gamma} \frac{1}{2} I(\psi), \quad (6)$$

where $\langle\sigma v\rangle$ is the annihilation cross section times the relative velocity mediated over the galactic velocity distribution function, and dN_γ/dE_γ is the energy spectrum of γ -rays originated from a single DM pair annihilation. In particular, we may identify WIMP candidates with neutralinos in the Minimal Supersymmetric Standard Model (see Ref. [47] and refs. therein).

The photon spectrum in the continuum originates from the production of fermions, gauge bosons, Higgs bosons, and gluons from the annihilation of WIMP pairs. The spectra dN_γ/dE_γ from DM final states into $b\bar{b}$, $\mu^+\mu^-$ and $\tau^+\tau^-$ have been taken from Refs. [48, 49].

The quantity $I(\psi)$ is the integral performed along the l.o.s. of the squared DM density distribution:

$$I(\psi) = \int_{l.o.s.} \rho^2(r(\lambda, \psi)) d\lambda. \quad (7)$$

with ψ being the angle between the l.o.s. and the direction pointing toward the galactic center (GC) and defined in function of the galactic coordinates so that $\cos\psi = \cos b \cos l$. When comparing with experimental data, Eq. (7) must be averaged over the telescope observing solid angle, $\Delta\Omega$:

$$I_{\Delta\Omega} = \frac{1}{\Delta\Omega} \int_{\Delta\Omega} I(\psi(b, l)) d\Omega. \quad (8)$$

The integral of the squared DM density over the line-of-sight depends from the choice on $\rho(r)$. When including the galactic center in the integration (Eq. (7)), different DM distributions may lead to very different results for $I(\psi)$. However, since our analysis is applied to high latitude regions, the various descriptions for $\rho(r)$ point to very similar values for $I(\psi)$. We neglect any clumpiness effects and assume a smooth distribution of DM in the galactic halo. The results for $I_{\Delta\Omega}$ for different DM den-

Halo profile	Isothermal a = 3.5 kpc	NFW [50] a = 25 kpc $r_c = 0.01$ pc	Einasto [51] $\alpha = 0.142$ $r_{-2} = 26.4$ pc $\rho_{-2} = 0.05$ GeV cm $^{-3}$
$ b > 10^\circ$	2.389	2.400	2.833
$10^\circ < b < 20^\circ$	4.020	4.166	5.752
$ b > 60^\circ$	1.226	1.283	1.232

TABLE I: Values for $I_{\Delta\Omega}$ in units of GeV 2 cm $^{-6}$ kpc. For all these profiles $\rho_l = 0.4$ GeV cm $^{-3}$, $R_{Sun} = 8.2$ kpc.

sity distributions and observational regions are reported in Table I. All the DM profiles provide very similar results for latitudes well above the galactic plane. Hereafter, the results will be provided for the cored isothermal density profile.

B. Results on annihilation cross section

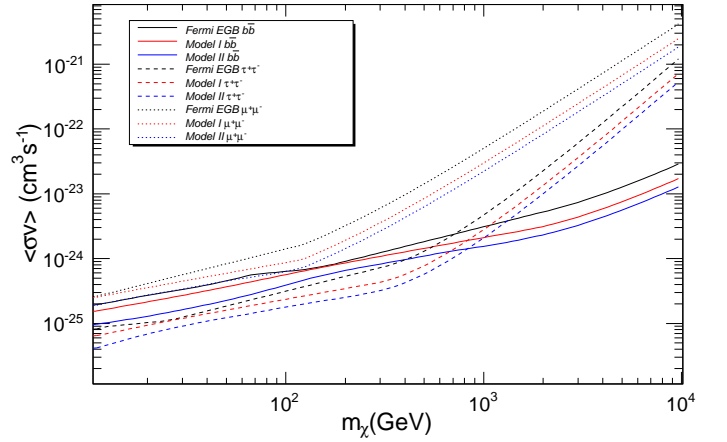


FIG. 3: Upper bounds on the thermal annihilation DM cross section from γ -ray in the high latitude galactic halo, as a function of the DM mass. From top to bottom, solid lines refer to limits on $\langle\sigma v\rangle$ from the comparison with the EGB as derived by the Fermi-LAT Collaboration [7] (black lines), Model I (red lines) and Model II (blue lines). Dotted, solid and dashed lines correspond DM annihilation into $\mu^+\mu^-$, $b\bar{b}$, $\tau^+\tau^-$, respectively.

In Fig. 3 we display the conservative upper bounds on the thermal annihilation DM cross section, derived within the previous assumptions. From top to bottom solid lines refers to the limits on $\langle\sigma v\rangle$ arising from the comparison with the EGB derived by the Fermi-LAT Collaboration [7] (black line) and our Model I (red line) and Model II (blue line). Given the scaling of the DM flux $\propto m_\chi^2$, $\langle\sigma v\rangle$ is increasing with the mass and spans about two orders of magnitude in the considered mass interval.

The dip in the solid upper curve traces the change of the energy bin relevant for the derivation of the limits on $\langle\sigma v\rangle$. Moreover the limits arising from the Fermi-LAT EGB and the conservative residual are similar in the range of masses $\simeq 100 - 200$ GeV, for which the bounds on $\langle\sigma v\rangle$ arise from energy $\simeq 8 - 9$ GeV, where the contribution of MSPs falls down avoiding a significant reduction of the residual EGB with respect to the Fermi-EGB. The Fermi-LAT data for the EGB are available also for latitudes $10^\circ < |b| < 20^\circ$ and $|b| > 60^\circ$ [7]. The flux in Eq. (6) changes for the mere normalization factors given in Table I. However, given the intensity of the measured fluxes our upper limits do not change if derived for the other high latitude regions.

We emphasize that our limits are almost model independent: little dependence on the DM distribution, being at high latitudes, and mild differences due to final states. Our limits are *conservative*: it is very unlikely that a higher signal be compatible with Fermi EGB. Similarly, our upper limits could be lowered only with assumptions on non-homogeneous DM distributions.

C. Bounds on the Sommerfeld enhancement for $\langle\sigma v\rangle$

Recent claims on the excess of CR positrons [1] have stimulated the interpretation of data in terms of annihilating DM with fairly large annihilation cross sections of the order of $10^{-23} - 10^{-22}$ cm³/s. These numbers are at least three orders of magnitude larger than the value indicated by observations of the DM abundance due to thermal production. One way to boost the annihilation cross section is through the Sommerfeld effect [14, 52–56], generically due to an attractive force acting between two particles, *i.e.* a Yukawa or a gauge interaction. In the case of DM particles, the main effect of such an attractive force would be to enhance $\langle\sigma v\rangle$ by a factor proportional to $1/\beta = c/v$, where v is the velocity of the DM particle ($1/v$ enhancement). The net result on the annihilation cross section writes as $\langle\sigma v\rangle_S = S \langle\sigma v\rangle$, where S sizes the Sommerfeld enhancement of the annihilation amplitude. We have evaluated the Sommerfeld enhancement S using the approximation of the Yukawa potential by the Hulthen potential, for which an analytic solution is possible [57, 58] (and checked that the solution coincides with the numerical one). The Sommerfeld enhancement factor behaves as $1/v$ and for very small velocities it saturates to constant values. Given α the coupling constant and m_ϕ the mass of the new force carrier, if the quantity $m_\phi/m_\chi \cdot \alpha$ is close to the values that make the Yukawa potential have zero-energy bound states, the enhancement is much larger; indeed, the enhanced cross section shows resonances at $m_\chi = \frac{4m_\phi n^2}{\alpha}$ ($n = 1, 2, 3, \dots$), which grow as $1/v^2$, up to the point where they get cut off by finite width effects.

In Fig. 4 we show the Sommerfeld enhanced cross sections for $\alpha = \frac{1}{4\pi}$, $\beta = 10^{-8}$ and a force carrier of mass

$m_\phi = 1$ GeV (upper curve) and $m_\phi = 90$ GeV (lower curve). We over-impose the upper bounds obtained in the previous Section from the residual EGB Model I and Model II and already displayed in Fig. 3. Our results show that a Sommerfeld enhancement due to a force carrier of $m_\phi < 1$ GeV ($\alpha = \frac{1}{4\pi}$) is strongly excluded by Model I and II for the Fermi-LAT EGB data. For a massive force carrier (90 GeV) only the resonant peaks above the TeV mass are excluded. The result holds for $\beta = 10^{-8}$ up to $\beta = 10^{-3}$.

Therefore, high latitude γ -ray observations interpreted as due to DM annihilation in the Milky Way halo bound the Sommerfeld enhancement of the annihilation cross section to a factor of 3-10-50-200 for $m_\chi=10$ -100-1000-5000 GeV, respectively. In case a Yukawa-like potential describes this non-relativistic quantum effect, a force carrier heavier than 1 GeV is definitely required.

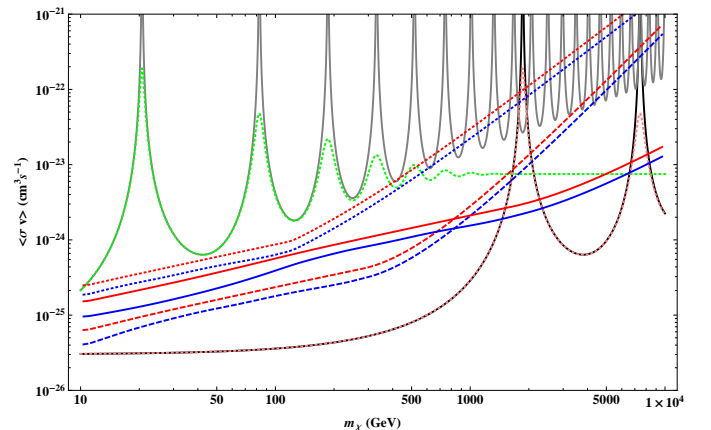


FIG. 4: Sommerfeld enhancement of the annihilation cross section as a function of the DM mass, for $\alpha = \frac{1}{4\pi}$. Solid curves are for $\beta = 10^{-8}$, dotted ones for $\beta = 10^{-3}$. The upper (lower) resonant curve is obtained for a force carrier of mass $m_\phi = 1$ GeV (90 GeV). The upper (lower) dotted, solid and dashed curves correspond to the upper bounds for EGB Model I (Model II) derived from WIMPs annihilating in the high latitude galactic halo in $\mu^+\mu^-$, $b\bar{b}$, $\tau^+\tau^-$, respectively (see Fig. 3.)

D. Bounds from the high-redshift protohalos

A possible way to boost the annihilation rate is to modify the particle theory and make the ansatz that the annihilation cross section depends on the inverse of the velocity. A boosted production of γ -rays in models with $\langle\sigma v\rangle \propto 1/v$ has been proposed for the first bound objects formed in the early phases of the universe [59, 60]. After the matter-radiation equality is reached, DM perturbations start growing via gravitational instability and form the first bound protohalos at a redshift of about 140. The birth of these protohalos depends on the properties of the DM particles, since they are responsible of the primor-

dial inhomogeneities. The complete decoupling of DM particles from the thermal bath happens therefore quite later with respect to the freeze-out temperature T_f , at a temperature of kinetic decoupling T_{kd} which sets the distance scale at which linear density perturbations in the DM distributions are wiped off. This small-scale cutoff in the matter power spectrum sets in turn the mass M_c of the primordial DM structures. Since the T_{kd} establishes the link between the first halos' mass and the DM nature, it is heavily depending on the WIMP model and on assumptions about the WIMP interactions. Notably, the DM particle cross section for scattering off Standard Model particles, sets the time of both its thermal and kinematic decoupling from cosmic plasma. The velocity dispersion of the first protohalos that collapse at redshift z_C is estimated to be very small ($\beta \sim 10^{-8}$). Therefore, models for $\langle\sigma v\rangle$ depending on the inverse of v predict a boosted flux of DM annihilation products. The photons arising from WIMP annihilations in very early halos can freely propagate with their energy red-shifting and reach the Earth in the range $\sim \text{keV} - \text{TeV}$, while photons emitted out of this transparency window are absorbed by the intergalactic medium and can be observed in principle through their interactions with the CMB. The $1/v$ enhancement of the annihilation cross section may be simply parameterized by writing [60]:

$$\langle\sigma v\rangle = \langle\sigma v\rangle_0 \frac{c}{v} \text{ cm}^3/\text{s}. \quad (9)$$

The energy density in photons today from WIMP annihilation in the primordial halos can be theoretically predicted by:

$$\rho_\gamma = 5.28 \cdot 10^6 \left(\frac{M_c}{M_\oplus} \right)^{-1/3} \langle\sigma v\rangle_0 B_{2.6} \left(\frac{m_\chi}{\text{TeV}} \right)^{-1} \text{ GeV cm}^{-3}, \quad (10)$$

where the cosmological boost factor B , normalized to 2.6 ($B_{2.6} = B/2.6$) takes into account that the DM is distributed according to a Navarro-Frenk-White (NFW) density profile with the lowest concentration parameter [60]. Eq. (10) can be compared with the experimental photon density inferred for the Fermi-LAT EGB [7] and for our two EGB models derived in Sect. II A, which is obtained by integrating the photon flux on the Fermi-LAT energy range (100 MeV - 100 GeV). We obtain:

$$\rho_\gamma \simeq 6.62 \cdot 10^{-16} \left(\frac{E_\gamma}{\text{GeV}} \right)^{-0.41} \text{ GeV cm}^{-3} \text{ (Fermi - LAT)} \quad (11)$$

$$\rho_\gamma \simeq 5.65 \cdot 10^{-16} \left(\frac{E_\gamma}{\text{GeV}} \right)^{-0.41} \text{ GeV cm}^{-3} \text{ (Model I)} \quad (12)$$

$$\rho_\gamma \simeq 4.5 \cdot 10^{-16} \left(\frac{E_\gamma}{\text{GeV}} \right)^{-0.46} \text{ GeV cm}^{-3} \quad (13)$$

(Model II, $E_\gamma > 8 \text{ GeV}$)

We constrain $\langle\sigma v\rangle_0$ by comparison of the theoretical expression 10 with the experimental γ -ray density. The results are displayed in Fig. 5 as a function of the WIMP mass. The three central lines bound the $\langle\sigma v\rangle_0$ (Eq. (9)) parameter from Fermi-LAT photon density given in Eq. (11), Eq. (12) and Eq. (14) respectively, from top to bottom, when $M_c = M_\oplus$. The upper (dotted) and the lower (dashed) bounds are derived for Model II when $M_c = 10^2 M_\oplus$ (upper) and $10^{-2} M_\oplus$ (lower). The bounds on $\langle\sigma v\rangle_0$ are strong: for WIMP masses below 100 GeV it is forced to be $< 10^{-33} \text{ cm}^3/\text{s}$. Upper bounds grow to $< 10^{-32} \text{ cm}^3/\text{s}$ for $m_\chi \simeq 1 \text{ TeV}$ and sets to $< 10^{-31} \text{ cm}^3/\text{s}$ at 10 TeV. We make notice that they are more stringent than limits obtained from primordial light elements abundance and CMB anisotropies [61].

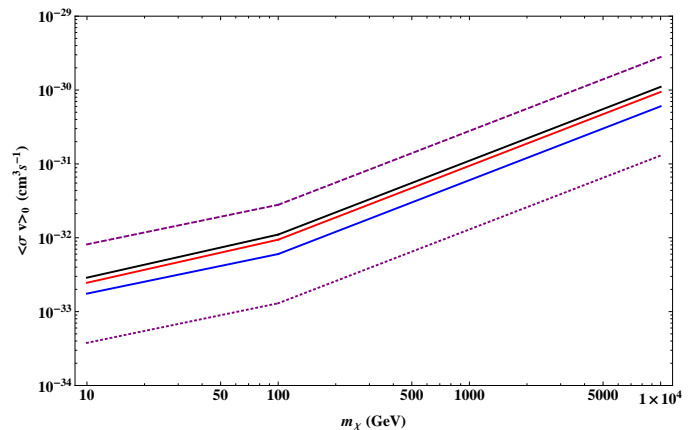


FIG. 5: Bounds on $\langle\sigma v\rangle_0$ from Eq. (9), as a function of the DM mass. The central three bounds are obtained for $M_c = M_\oplus$, and from Eqs. (11) (black line), (12) (red line) and (14) (blue line) respectively, from top to bottom. The upper (lower) purple lines are derived from Eq. (14) for Model II EGB and $M_c = 10^2 M_\oplus$ ($10^{-2} M_\oplus$).

The $1/v$ behaviour of the $\langle\sigma v\rangle$ may be identified with the Sommerfeld effect for velocities $\beta \gg (m_\phi/m_\chi)^{1/2}$ [53]. For lower velocities, as are the ones typical for protohalos, the series of resonances appears (see Sect. III C) and the Sommerfeld enhancement S behaves as $1/v^2$ close to the peaks. In this case, the upper bounds on the annihilation cross section may be obtained by rescaling $\langle\sigma v\rangle = \langle\sigma v\rangle_0 S$ with a factor $1/\beta \cdot m_\phi/m_\chi$. From Eqs. 10 - 14 it is straightforward to notice that the bounds on a Sommerfeld enhanced $\langle\sigma v\rangle$ derived from an overproduction of γ -rays in protohalos, are much weaker than the ones imposed by annihilation in the high-latitude galactic halo.

IV. CONCLUSIONS

The γ -ray EGB measured by Fermi-LAT [7] likely includes contributions from galactic and extragalactic *unresolved* sources. We have explored possible non-

negligible diffuse contributions from unresolved blazars, MSPs, star-forming galaxies and UHECRs. Lead by a conservative attitude, we have considered the minimal contribution for all sources, and neglected those objects whose high latitude flux is not excluded to be less than 1% of Fermi-LAT EGB. Two residual EGB fluxes have been derived by subtraction of the additional fluxes from the Fermi-LAT EGB: Model I is obtained after the subtraction of unresolved BL Lacs, FSRQs and galactic MSPs, while Model II is the residual flux after the further subtraction of star-forming galaxies and UHECRs. From our new residual EGB fluxes, we have set upper limits on the DM annihilation cross section into γ -rays. A conservative upper bound on $\langle\sigma v\rangle$ is derived by assuming that the Model I and II EGB are entirely due to WIMPs pair-annihilating in the halo of our Galaxy. Values for $\langle\sigma v\rangle \gtrsim 10^{-25} \text{ cm}^3/\text{s}$ are strongly excluded for $m_\chi \simeq 10 \text{ GeV}$, while for $m_\chi \simeq 100 \text{ GeV}$ (1 TeV) the annihilation rate is bounded to $3 \cdot 10^{-25} \text{ cm}^3/\text{s}$ ($10^{-24} \text{ cm}^3/\text{s}$). This results holds for DM annihilating into $b\bar{b}$. Stronger limits below $m_\chi = 1 \text{ TeV}$ are derived for annihilation into the leptonic τ annihilating channel, while for the μ channel the limits are close to the $b\bar{b}$ below $m_\chi = 100 \text{ GeV}$, and weaker above this mass. Annihilation into leptons is therefore excluded at a level which strongly disfavours the interpretation of cosmic positron fraction data in terms of leptophilic DM with small cosmological boost factors. The latter boost factors are in turns strongly limited by antiproton data [8].

The bounds on $\langle\sigma v\rangle$ have been interpreted in terms of Sommerfeld enhancement of the annihilation cross section. A Sommerfeld enhancement due to a force carrier of $m_\phi < 1 \text{ GeV}$ ($\alpha = \frac{1}{4\pi}$) is strongly excluded by Model I and II for the Fermi-LAT EGB data. For a massive force carrier (90 GeV) only the resonant peaks

above the TeV mass are excluded. High latitude γ -ray observations interpreted as due to DM annihilation in the Milky Way halo bound the Sommerfeld enhancement of the annihilation cross section to a factor of 3-10-50-200 for $m_\chi = 10-100-1000-5000 \text{ GeV}$, respectively, and in case an annihilation into light quarks occurs. For $m_\chi \lesssim 6-700 \text{ GeV}$ these limits are reduced by a factor of few for the pure $\tau^+\tau^-$ annihilation channel. In case a Yukawa-like potential describes this non-relativistic quantum effect, a force carrier heavier than 1 GeV is definitely required. Finally, we have explored the possibility that the residual γ -ray EGB is entirely due to cosmological annihilation of DM in protohalos at high redshift. Within the hypothesis that $\langle\sigma v\rangle$ is inversely proportional to the WIMP velocity, very severe limits are derived for the velocity-independent part of the annihilation cross section, depending on the protohalo mass.

V. ACKNOWLEDGEMENTS

We warmly thank M. Ajello and L. Latronico for helpful comments on sources in the Fermi catalog. We are grateful to Torsten Bringmann for fruitful discussions and suggestions. F.C. thanks Vlasios Vasileiou and the Astrophysics Science Division of the NASA's Goddard Space Flight Center, where part of this work was done within the ISSNAF - INAF Internship Program 2010. This work was supported by the EU grant UNILHC PITN-GA-2009-237920, by the Spanish MICINN under grants FPA2008-00319/FPA, by the MULTIDARK Consolider CSD2009-00064, by Prometeo/2009/091. F.C. acknowledges support from the German Research Foundation (DFG) through grant BR 3954/1-1.

-
- [1] O. Adriani, G. C. Barbarino, G. A. Bazilevskaya, R. Bellotti, M. Boezio, E. A. Bogomolov, L. Bonechi, M. Bongi, V. Bonvicini, S. Bottai, et al., *Nature (London)* **458**, 607 (2009), 0810.4995.
 - [2] O. Adriani, G. C. Barbarino, G. A. Bazilevskaya, R. Bellotti, M. Boezio, E. A. Bogomolov, L. Bonechi, M. Bongi, V. Bonvicini, S. Borisov, et al., *Astropart. Phys.* **34**, 1 (2010), 1001.3522.
 - [3] A. A. Abdo, M. Ackermann, M. Ajello, W. B. Atwood, M. Axelsson, L. Baldini, J. Ballet, G. Barbiellini, D. Bastieri, M. Battelino, et al., *Phys. Rev. Lett.* **102**, 181101 (2009), 0905.0025.
 - [4] F. Aharonian, A. G. Akhperjanian, G. Anton, U. Barres de Almeida, A. R. Bazer-Bachi, Y. Becherini, B. Behera, K. Bernlöhner, A. Bochow, C. Boisson, et al., *Astron. Astrophys.* **508**, 561 (2009), 0905.0105.
 - [5] O. Adriani, G. C. Barbarino, G. A. Bazilevskaya, R. Bellotti, M. Boezio, E. A. Bogomolov, L. Bonechi, M. Bongi, V. Bonvicini, S. Bottai, et al., *Phys. Rev. Lett.* **102**, 051101 (2009), 0810.4994.
 - [6] O. Adriani et al. (PAMELA), *Phys. Rev. Lett.* **105**, 121101 (2010), 1007.0821.
 - [7] A. A. Abdo, M. Ackermann, M. Ajello, W. B. Atwood, L. Baldini, J. Ballet, G. Barbiellini, D. Bastieri, et al., *Phys. Rev. Lett.* **104**, 101101 (2010), 1002.3603.
 - [8] F. Donato, D. Maurin, P. Brun, T. Delahaye, and P. Salati, *Phys. Rev. Lett.* **102**, 071301 (2009), 0810.5292.
 - [9] W. Mitthumsiri, *Fermi Symposium, Rome* (2011).
 - [10] T. Delahaye, J. Lavalle, R. Lineros, F. Donato, and N. Fornengo, *Astron. Astrophys.* **524**, A51 (2010), 1002.1910.
 - [11] D. Hooper, P. Blasi, and D. Serpico, *JCAP* **1**, 25 (2009), 0810.1527.
 - [12] M. Cirelli, R. Franceschini, and A. Strumia, *Nuclear Phys. B* **800**, 204 (2008), 0802.3378.
 - [13] L. Bergström, T. Bringmann, and J. Edsjö, *Phys. Rev. D* **78**, 103520 (2008), 0808.3725.
 - [14] N. Arkani-Hamed, D. P. Finkbeiner, T. R. Slatyer, and N. Weiner, *Phys. Rev. D* **79**, 015014 (2009), 0810.0713.
 - [15] I. Cholis, L. Goodenough, D. Hooper, M. Simet, and N. Weiner, *Phys. Rev. D* **80**, 123511 (2009).

- [16] A. A. Abdo, M. Ackermann, M. Ajello, W. B. Atwood, L. Baldini, J. Ballet, G. Barbiellini, D. Bastieri, K. Bechtol, R. Bellazzini, et al., *Astrophys. J.* **712**, 147 (2010), 1001.4531.
- [17] M. Ackermann, M. Ajello, A. Allafort, L. Baldini, J. Ballet, G. Barbiellini, D. Bastieri, K. Bechtol, R. Bellazzini, R. D. Blandford, et al., *JCAP* **5**, 25 (2010), 1002.2239.
- [18] A. A. Abdo, M. Ackermann, M. Ajello, L. Baldini, J. Ballet, G. Barbiellini, D. Bastieri, K. Bechtol, R. Bellazzini, B. Berenji, et al., *JCAP* **4**, 14 (2010).
- [19] A. A. Abdo, M. Ackermann, M. Ajello, W. B. Atwood, L. Baldini, J. Ballet, G. Barbiellini, D. Bastieri, K. Bechtol, R. Bellazzini, et al., *Phys. Rev. Lett.* **104**, 091302 (2010), 1001.4836.
- [20] A. A. Abdo et al., *Astrophys. J.* **188**, 405 (2010).
- [21] A. A. Abdo, M. Ackermann, M. Ajello, E. Antolini, L. Baldini, J. Ballet, G. Barbiellini, D. Bastieri, B. M. Baughman, K. Bechtol, et al., *Astrophys. J.* **720**, 435 (2010), 1003.0895.
- [22] A. A. Abdo, M. Ackermann, M. Ajello, W. B. Atwood, M. Axelsson, L. Baldini, J. Ballet, G. Barbiellini, M. G. Baring, D. Bastieri, et al., *Astrophys. J. Suppl.* **187**, 460 (2010), 0910.1608.
- [23] B. D. Fields, V. Pavlidou, and T. Prodanovic, *Astrophys. J. Lett.* **722**, L199 (2010), 1003.3647.
- [24] O. Kalashev, D. Semikoz, and G. Sigl, *Phys. Rev. D* **79**, 063005 (2009).
- [25] Y. Inoue, T. Totani, and Y. Ueda, *Astrophys. J.* **672**, L5 (2008).
- [26] Y. Inoue and T. Totani, *Astrophys. J.* **702**, 523 (2009).
- [27] A. A. Abdo, M. Ackermann, M. Ajello, L. Baldini, J. Ballet, G. Barbiellini, D. Bastieri, K. Bechtol, R. Bellazzini, B. Berenji, et al., *Astrophys. J.* **720**, 912 (2010).
- [28] L. Stawarz and T. M. Kneiske, *Astrophys. J.* **637**, 693 (2006).
- [29] Y. Inoue, *ArXiv e-prints* (2011), 1103.3946.
- [30] T. Le and C. D. Dermer, *Astrophys. J.* **700**, 10261033 (2009).
- [31] A. A. Abdo, M. Ackermann, M. Ajello, W. B. Atwood, L. Baldini, J. Ballet, G. Barbiellini, et al., *Astrophys. J. Lett.* **709**, L152 (2010).
- [32] T. A. Thompson, E. Quataert, and E. Waxman, *Astrophys. J.* **654**, 219 (2006).
- [33] P. Blasi, S. Gabici, and G. Brunetti, *Int. J. Mod. Phys. A* **22**, 681 (2007).
- [34] R. C. Berrington and C. D. Dermer, *Astrophys. J.* **594**, 709 (2003).
- [35] C. Pfrommer et al., *MNRAS* **385**, 1211 (2008).
- [36] U. Keshet, E. Waxman, A. Loeb, et al., *Astrophys. J.* **585**, 128 (2003).
- [37] S. Gabici and P. Blasi, *Astropart. Phys.* **19**, 679 (2003).
- [38] P. Sreekumar et al., *Astrophys. J.* **494**, 523 (1998).
- [39] F. W. Stecker and T. M. Venters (2010), 1012.3678.
- [40] C. A. Faucher-Giguere and A. Loeb, *JCAP* **1001**, 005 (2010).
- [41] J. M. Siegal-Gaskins, R. Reesman, V. Pavlidou, S. Profumo, and T. P. Walker, *ArXiv e-prints* (2010), 1011.5501.
- [42] A. A. Abdo et al., *Science* **325**, 848 (2009).
- [43] R. Makika et al., *Astrophys. J.* **728**, 158 (2011), 1005.1390.
- [44] V. Berezhinsky, A. Gazizov, M. Kachelriess, and S. Ostapchenko, *Phys. Lett. B* **695**, 13 (2010), 1003.1496.
- [45] H. Bengtsson, P. Salati, and J. Silk, *Nuclear Phys. B* **346**, 129 (1990).
- [46] L. Bergström, P. Ullio, and J. H. Buckley, *Astropart. Phys.* **9**, 137 (1998), 9712318.
- [47] A. Bottino, F. Donato, N. Fornengo, and S. Scopel, *Phys. Rev. D* **70**, 015005 (2004), 0401186.
- [48] N. Fornengo, L. Pieri, and S. Scopel, *Phys. Rev. D* **70**, 103529 (2004), 0407342.
- [49] J. A. R. Cembranos, A. de La Cruz-Dombriz, A. Dobado, R. A. Lineros, and A. L. Maroto, *Phys. Rev. D* **83**, 083507 (2011), 1009.4936.
- [50] J. F. Navarro, C. S. Frenk, and S. D. M. White, *Astrophys. J.* **462**, 563 (1996).
- [51] J. F. Navarro, E. Hayashi, C. Power, A. R. Jenkins, C. S. Frenk, S. D. M. White, V. Springel, J. Stadel, and T. R. Quinn, *MNRAS* **349**, 1039 (2004), 0311231.
- [52] A. J. W. Sommerfeld, *Annalen der Physik* **403** (1931).
- [53] M. Lattanzi and J. Silk, *Phys. Rev. D* **79**, 083523 (2009), 0812.0360v2.
- [54] J. Hisano, S. Matsumoto, and M. M. Nojiri, *Phys. Rev. Lett.* **92**, 1 (2004), 037216v1.
- [55] R. Iengo, *JHEP* **0905:024**, 1 (2009), 0902.0688.
- [56] J. Zavala, M. Vogelsberger, T. R. Slatyer, A. Loeb, and V. Springel, accepted for publication in *Phys. Rev. D* (2011), 1103.0776.
- [57] S. Cassel, *Journal of Physics G Nuclear Physics* **37**, 105009 (2010), 0903.5307.
- [58] J. L. Feng, M. Kaplinghat, and H.-B. Yu, *Phys. Rev. D* **82**, 083525 (2010), 1005.4678v1.
- [59] S. Profumo, K. Sigurdson, and M. Kamionkowski, *Phys. Rev. Lett.* **97**, 1 (2006), 0603373v1.
- [60] S. Profumo and M. Kamionkowski, *Phys. Rev. Lett.* **10**, 261301 (2008), 0810.3233.
- [61] J. Hisano, M. Kawasaki, K. Kohri, T. Moroi, K. Nakayama, and T. Sekiguchi (2011), 1102.4658.